Inorganic Chemistry

ARTICLE

pubs.acs.org/IC

Chemical Reactivity and Electrochemistry of Metal−Metal-Bonded Zincocenes

Mario Carrasco,[†] Riccardo Peloso,[†] Irene Resa,[†] Amor Rodríguez,[†] Luis Sánchez,[†] Eleuterio Álvarez,[†] Celia Maya,[†] Rafael Andreu,*[,‡] Juan José Calvente,[‡] Agustín Galindo,[§] and Ernesto Carmona*[,†]

[†]Instituto de Investigaciones Químicas-Departamento de Química Inorgánica, Universidad de Sevilla-Consejo Superior de Investigaciones Científicas, Avenida Américo Vespucio 49, 41092 Sevilla, Spain

[‡]Departamento de Química Física, Facultad de Química, Universidad de Sevilla, 41012 Sevilla, Spain

[§]Departamento de Química Inorgánica, Facultad de Química, Universidad de Sevilla, 41012 Sevilla, Spain

Supporting Information

ABSTRACT: Attempts to prepare mixed-ligand zinc−zinc-bonded compounds that contain bulky C_5Me_5 and terphenyl groups, $[Zn_2(C_5Me_5)(Ar')]$, lead to disproportionation. The resulting half-sandwich Zn(II) complexes $[(\eta^5\text{-}C_5Me_5)ZnAr']$ (Ar′ = 2,6-(2,6-^{i}Pr$_2$C$_6$H$_3$)$_2$-C$_6$H$_3$, **2**; 2,6-(2,6-Me$_2$C$_6$H$_3$)$_2$-C$_6$H$_3$, **3**) can also be obtained from the reaction of $[Zn(C_5Me_5)_2]$ with the corresponding LiAr′. In the presence of pyr-py (4-pyrrolidinopyridine) or DBU (1,8-diazabicyclo[5.4.0]undec-7-ene), $[Zn_2(\eta^5\text{-}C_5Me_5)_2]$ reacts with C_5Me_5OH to afford the tetrametallic complexes $[Zn_2(\eta^5\text{-}C_5Me_5)L(\mu\text{-}OC_5Me_5)]_2$ (L = pyr-py, **6**; DBU, **8**), respectively. The bulkier terphenyloxide $Ar^{Mes}O^-$ group (Ar^{Mes} = 2,6-(2,4,6-Me$_3$C$_6$H$_2$)$_2$-C$_6$H$_3$) gives instead the dimetallic compound $[Zn_2(\eta^5\text{-}C_5Me_5)(OAr^{Mes})(pyr\text{-}py)_2]$, **7**, that features a terminal Zn−OAr^{Mes} bond. DFT calculations on models of **6**−**8** and also on the Zn−Zn-bonded complexes $[Zn_2(\eta^5\text{-}C_5H_5)(OC_5H_5)(py)_2]$ and $[(\eta^5\text{-}C_5H_5)ZnZn(py)_3]^+$ have been performed and reveal the nonsymmetric nature of the Zn−Zn bond with lower charge and higher participation of the s orbital of the zinc atom coordinated to the cyclopentadienyl ligand with respect to the metal within the pseudo-ZnL$_3$ fragment. Cyclic voltammetric studies on $[Zn_2(\eta^5\text{-}C_5Me_5)_2]$ have been also carried out and the results compared with the behavior of $[Zn(C_5Me_5)_2]$ and related magnesium and calcium metallocenes.

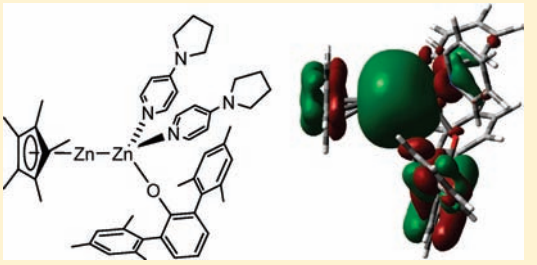

INTRODUCTION

Close to the 60th anniversary of the discovery of ferrocene and recognition of its characteristic sandwich structure,[1] metallocenes continue to attract a great deal of interest due to their numerous and important applications in different areas of chemistry.[2,3] Bulky, substituted cyclopentadienyl ligands have had a tremendous impact in metallocene chemistry and have, inter alia, triggered the study of metallocenes of the main group elements.[4]

A remarkable structural variety has been uncovered for this metallocene group, from which zincocenes do not escape. Thus, although molecular zinc metallocenes, $ZnCp'_2$ (Cp′ denotes a cyclopentadienyl ligand), feature a slipped-sandwich structure with η^5- and $\eta^1(\pi)$-Cp′ ligands, a common structural characteristic of zincocenes is the low hapticity their Cp′ rings exhibit,[5] frequently η^1 or η^2. This is found, for instance, for the parent $ZnCp_2$ and related derivatives and also for anionic cyclopentadienyl zincates.[6] Expanding this diversity and contrasting with the low hapticity of Zn(II) metallocenes, the recently reported $[Zn_2(\eta^5\text{-}C_5Me_5)_2]$ and $[Zn_2(\eta^5\text{-}C_5Me_4Et)_2]$ present η^5-coordination of the Cp′ ligands and a directly bonded dizinc unit, which elevates them to a unique position, not only within the zincocene family but among all known metallocenes.[7]

A flurry of theoretical and experimental studies followed the synthesis of $[Zn_2(\eta^5\text{-}C_5Me_5)_2]$ (**1**), providing a clear picture of the, until then, unknown Zn−Zn bond and expanding significantly the number of well-defined compounds of this sort.[8−10] The Zn_2^{2+} unit of these molecules is kinetically stabilized toward disproportionation to Zn(0) and Zn(II) by the presence of bulky terphenyl groups or by a variety of chelating N-containing ligands. Some of the latter have also proved successful to stabilize Mg−Mg bonds.[11] Comparatively less attention has been paid to disclose the chemical reactivity of these molecules, with the notable exception of work by the group of Schulz on the use of compound **1** as a precursor for other Zn−Zn-bonded compounds.[12,13]

At the time we started this work, only Zn−Zn-bonded compounds stabilized by metal coordination to C- or N-donor ligands were known. Our original interest[7] in analogous molecules containing O-donor ligands has led us to investigate the reactivity of **1** toward different alcohols and phenols. To complete our contribution to the knowledge of compounds of the $[Zn-Zn]^{2+}$ core, we report in full[14] synthetic efforts aimed at enlarging this family of complexes. Since despite the increasing

Received: April 20, 2011
Published: June 07, 2011

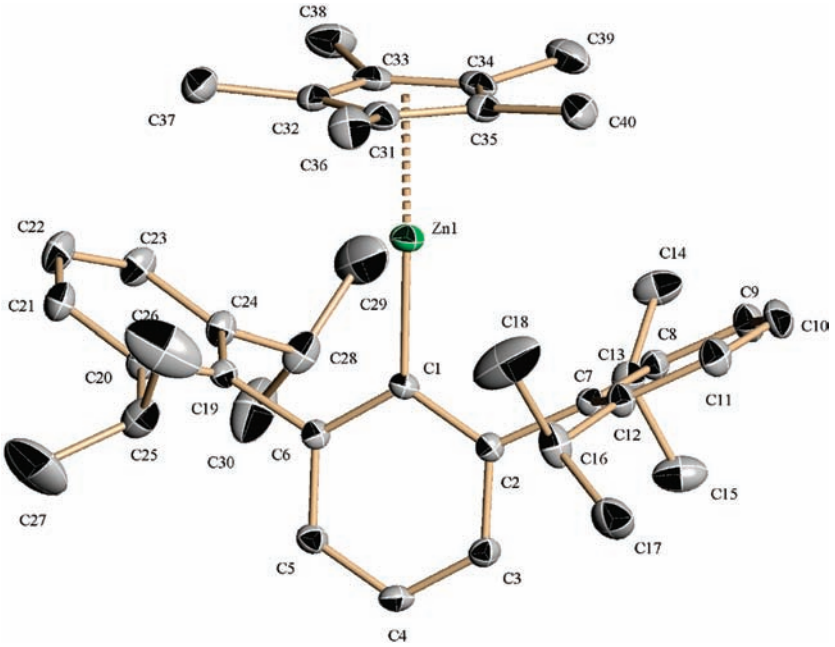

Figure 1. ORTEP representation for **2** (ellipsoids at 30% probability). Hydrogen atoms are not shown for clarity.

number of reports dealing with Zn−Zn-bonded compounds little or nothing has been made of their electrochemical properties, we deemed appropriate studying the electrochemistry of **1**. We describe it herein and compare it with properties of the related Zn(II) metallocene, $[Zn(C_5Me_5)_2]$, and of other $M(\eta^5\text{-}Cp')_2$ compounds of the alkaline-earth (Mg, Ca) and 3d metals (Mn, Fe).

RESULTS AND DISCUSSION

Synthesis and Reactivity of Zn−Zn-Bonded Complexes. Aiming at providing more insight into the reactivity that governs these unusual species, solutions of **1** and $Zn_2Ar'_2$[8a,b] (Ar′ = 2,6-(2,6-^{i}Pr$_2$C$_6$H$_3$)$_2$-C$_6$H$_3$) in deuterated benzene were combined and stirred for 24 h at room temperature. However, such reaction mixtures do not lead to the formation of new mixed-ligand complexes of formula Ar′ZnZnCp* (there is no trace of a new Zn−Zn-bonded product even when reflux conditions are applied for several hours). Alternatively, when **1** is reacted in diethyl ether with the lithium salts of the terphenyl ligands, LiAr′, precipitation of a dark pyrophoric solid with concomitant formation of soluble half-sandwich products $[(\eta^5\text{-}C_5Me_5)ZnAr']$ (Ar′ = 2,6-(2,6-^{i}Pr$_2$C$_6$H$_3$)$_2$-C$_6$H$_3$, **2**; 2,6-(2,6-Me$_2$C$_6$H$_3$)$_2$-C$_6$H$_3$, **3**) is observed (eq 1). In both cases, ^{1}H and ^{13}C{^{1}H} NMR spectroscopic data and FAB-MS analysis are consistent with the proposed formulation. The ^{1}H NMR spectra of **2** and **3** show sharp resonances due to the methyl protons of the Cp* rings at 1.64 and 1.62 ppm, respectively, with a high-field shift of about 0.4 ppm compared to $Zn_2Cp^*_2$. The ^{13}C nuclei of the Cp* moieties resonate very close to those of decamethyldizincocene.

$$[Zn_2(\eta^5\text{-}C_5Me_5)_2] + LiAr\prime \rightarrow [(\eta^5\text{-}C_5Me_5)ZnAr\prime] + Zn + LiCp^* \quad (1)$$

Clearly, a more convenient route for the preparation of **2** and **3** can be developed. Thus, reaction of $ZnCp^*_2$ with LiAr′ in Et$_2$O allows their isolation as analytically pure colorless solids with yields of 55% and 66%, respectively. Both compounds decompose readily when exposed to moisture and air but can be stored as solids under argon for months at room temperature. The molecular complexity of **2** has been confirmed by X-ray diffraction studies, revealing the expected half-sandwich structure and a congested metal−ligand environment, Figure 1. The Zn−C$_5$Me$_5$ coordination is similar to that found for the parent methyl derivative $[(\eta^5\text{-}C_5Me_5)ZnMe]$,[15] and it is characterized by a Zn−Cp*$_{centr}$ distance of 1.915 Å, whereas the Zn−C bond length to the terphenyl central aryl ring carbon atom of 1.960(2) Å is comparable to the Zn−CH$_3$ bond length of 1.943(5) Å. Additionally, the Zn−C$_{aryl}$ separation in **2** is identical within experimental error to Zn−C$_{aryl}$ bonds in other terphenyl zinc organometallics (for instance, 1.961(3) Å in (Ar′ZnI)$_2$ and ca. 1.97 Å in the metal−metal-bonded $Zn_2Ar'_2$).[8b]

Given the meager success of this approach for the synthesis of new dizincocenes, we pondered whether the use of bulky alkyl− and aryl−alcohols could lead to formation of the desired compounds through protonation of one of the cyclopentadienyl groups. Accordingly, the reactions of **1** with Ar^{Mes}OH (2,6-(2,4,6-Me$_3$C$_6$H$_2$)-C$_6$H$_3$OH) and C$_5$Me$_5$OH have been investigated. The reaction of **1** with Ar^{Mes}OH at low temperature (−20 °C) affords a white solid, whose insolubility makes typical solution NMR spectroscopy extremely difficult and prevents its characterization. Under similar conditions, C$_5$Me$_5$OH yields a complex mixture of unidentified products. Stabilization of the putative alkoxide (or aryloxide) derivatives by addition of pyridine does not prove feasible.[14] Having in mind Schulz's results regarding isolation of $[Cp^*Zn-Zn(dmap)_2Cp^*]$ by reaction of **1** with the more basic 4-dimethylaminopyridine, the related bases 4-pyrrolidinopyridine (pyr-py) and 1,8-diazabicyclo[5.4.0]undec-7-ene (DBU) have been employed. For comparative purposes, pK_a values for the conjugated acids of the above bases in acetonitrile are 12.53 (py), 17.95 (dmap), 18.33 (pyr-py), and 24.34 (DBU).[16]

In the absence of alcohol, a bright yellow solution forms immediately upon addition of 2 equiv of DBU to an ether

dx.doi.org/10.1021/ic200816f |*Inorg. Chem.* 2011, 50, 6361–6371

solution of **1**, indicating that coordination of the Lewis base has taken place. The newly formed compound is stable in solution for hours at room temperature, but it decomposes easily and rapidly as a solid forming a dark oily material. Due to its high instability all attempts to isolate this complex in the solid state have failed. However, this metal−metal-bonded adduct [Cp*Zn−Zn(DBU)$_2$Cp*] (**4**) can be unambiguously characterized by monitoring the reaction in deuterated benzene by ^{1}H and ^{13}C{^{1}H} NMR spectroscopy (see Experimental Section and below). On the other hand, when the synthesis of **4** is carried out in CH_2Cl_2, a colorless, air-stable compound forms, characterized by X-ray diffraction as the Zn(II) tetrahedral complex [ZnCl$_2$(DBU)$_2$] (see Supporting Information). This compound probably results from a radical reaction involving participation of CH_2Cl_2 that we have not investigated any further. Following the same procedure but replacing DBU by 4-pyrrolidinopyridine, the adduct [Cp*Zn−Zn(pyr-py)$_2$Cp*] (**5**) can be isolated. Compound **5** exhibits higher thermal stability than **4** and has been obtained as a pale yellow solid (see Experimental Section). Nevertheless, its extreme air and moisture sensitivity and its poor thermal stability make it very difficult to handle and purify, and no crystals suitable for X-ray diffraction analysis have been obtained. Spectroscopic data for the C_5Me_5 groups of these two compounds, **4** and **5**, are very similar to those reported by Schulz and co-workers for the dmap adduct [Cp*Zn−Zn(dmap)$_2$Cp*]. The ^{1}H NMR spectrum shows two singlets at 2.21 and 2.06 ppm, respectively (2.03 ppm in [Cp*Zn−Zn(dmap)$_2$Cp*]), due to the methyl protons of the cyclopentadienyl rings, along with the characteristic resonances of the DBU or pyr-py ligands. In the ^{13}C{^{1}H} NMR spectrum the C_5Me_5 methyl carbon nuclei resonate at 11.4 and 10.9 ppm, respectively, and are accompanied by a signal at 109.6 or 109.5 ppm, which corresponds to the quaternary carbon atoms of the cyclopentadienyl ring.

Compounds **4** and **5** can be seen as appropriate precursors to explore the possibility of preparing the targeted zinc−zinc-bonded compounds in the reaction with alcohols. The low-temperature (−60 °C) reaction of **5** (generated in situ from **1** and pyr-py at −10 °C) with 2,6-diisopropyl- and 2,6-dimethylphenol gives colorless solids that can be isolated after low-temperature workup. However, the two compounds are sparingly soluble in common solvents such as toluene or tetrahydrofuran. Furthermore, although they can be stored as solids for several days at −20 °C, they decompose upon attempted dissolution at temperatures above −40 °C. Hence, gathering meaningful spectroscopic data that would allow their characterization in solution has not proved feasible. These results suggest that bulkier RO$^-$ and ArO$^-$ groups are needed to stabilize an O-bound dizinc complex.

In accord with this hypothesis, use of Ar^{Mes}OH and C_5Me_5OH permits isolation and characterization of the targeted compounds. Thus, generation of **5** at −10 °C followed by its reaction with C_5Me_5OH at −25 °C yields a tetrametallic compound **6** (Scheme 1a) that consists of two Cp*ZnZn(pyr-py) units bridged by two $C_5Me_5O^-$ ligands. This complex, isolated as a colorless, very air-sensitive solid, can be indefinitely kept at −20 °C under inert atmosphere, although slow decomposition occurs at room temperature, particularly in solution. Characterization of this dimer has been achieved by low-temperature ^{1}H and ^{13}C{^{1}H} NMR spectroscopy and by X-ray crystallography.[14] As illustrated in Figure 2, the four Zn atoms and the two pyr-py N-donor atoms are practically coplanar. The

Scheme 1. Synthesis of Zn−Zn-Bonded Compounds Supported by Alkoxide and Aryloxide Ligands

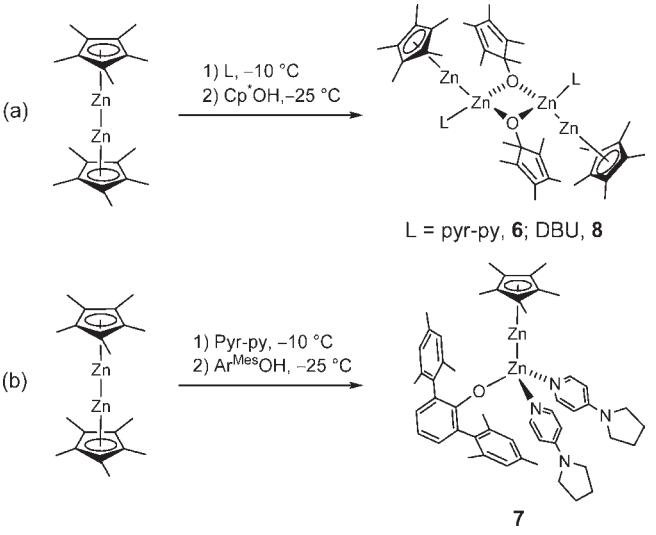

Zn−Zn bond, with a length of 2.366(1) Å, is longer than in **1** (2.31 Å) and comparable but somewhat shorter than in Zn_2Ar_2 (2.395(1) Å)[8a,b] and [Zn$_2$(C$_5$Me$_5$)$_2$(dmap)$_2$] (ca. 2.42 Å).[12a]

The analogous reaction with the bulkier terphenol Ar^{Mes}OH (Scheme 1b) proceeds similarly to yield a monomeric, bimetallic compound **7**, with superior thermal stability than **6**. It seems evident that the highly sterically demanding Ar^{Mes}O$^-$ unit prevents formation of a dimeric compound of type **6**. Solution NMR data for **7** indicate the additional incorporation of two pyr-py ligands. X-ray structure analysis (Figure 3) confirms this observation and preservation of the [Zn−Zn]$^{2+}$ moiety, which features a metal−metal bond of length 2.366(1) Å, which is identical within experimental error to that of **6**.

A third member of this family, compound **8**, that contains DBU as the stabilizing Lewis base, can be prepared similarly to **6** but employing DBU instead of pyr-py (Scheme 1a). Once again, a dimer of formulation [Zn$_2$(η^5-C$_5$Me$_5$)(μ-OC$_5$Me$_5$)(DBU)]$_2$ forms, in which the two Zn$_2$(η^5-C$_5$Me$_5$)(DBU) parts are bridged by the two alkoxide ligands. Complex **8** has a thermal stability comparable to **6** and is therefore lower than **7**, probably because of the steric hindrance exerted by the DBU ligands. This together with its poor solubility at low temperatures has prevented its full characterization by NMR methods (only the ^{1}H NMR has been recorded). Its molecular structure has been revealed by X-ray crystallography (Figure 2) and features Zn−Zn bonds with a length of ca. 2.39 Å.

Theoretical Calculations on Zn−Zn-Bonded Compounds. Prior to the synthesis of [Cp*Zn−Zn(dmap)$_2$Cp*] by Schulz and co-workers,[12a] all known dizinc compounds were homoleptic Zn$_2$L$_n$ complexes. Besides being a heteroleptic, nonsymmetric L$_n$ZnZnL′$_n$ derivative, Schulz's complex accommodates one of the Zn atoms of the dizinc moiety within a ML$_3$-type metal fragment. Since compounds **6**−**8** exhibit the same features, it was considered of interest to perform a DFT study.

From a qualitative point of view, the Zn−Zn bonding in **6**−**8** (and in other CpZnZnL$_3$ compounds) can be explained as resulting from the overlap of the two singly occupied HOMOs of (η^5-C$_5$R$_5$)Zn and ZnL$_3$ fragments. With reference to the classical MO diagrams of these fragments,[12] the SOMO of the

dx.doi.org/10.1021/ic200816f |Inorg. Chem. 2011, 50, 6361–6371

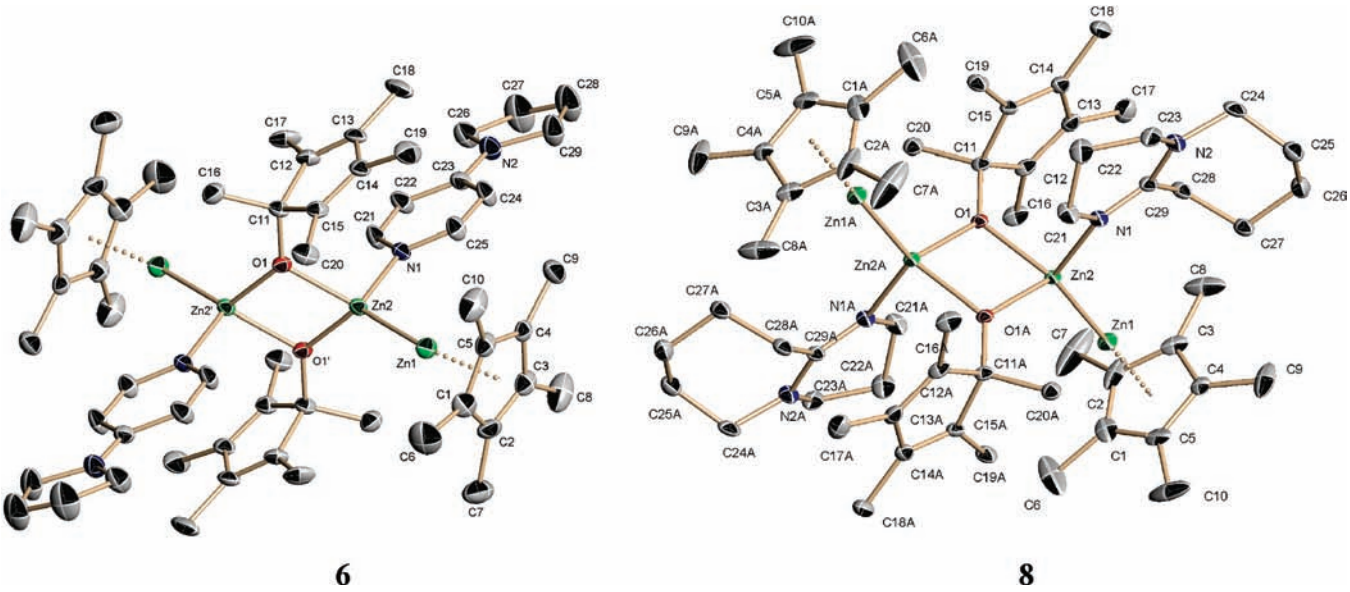

Figure 2. X-ray structures of complexes **6** and **8**, with hydrogen atoms omitted for clarity (ellipsoids at 30% probability).

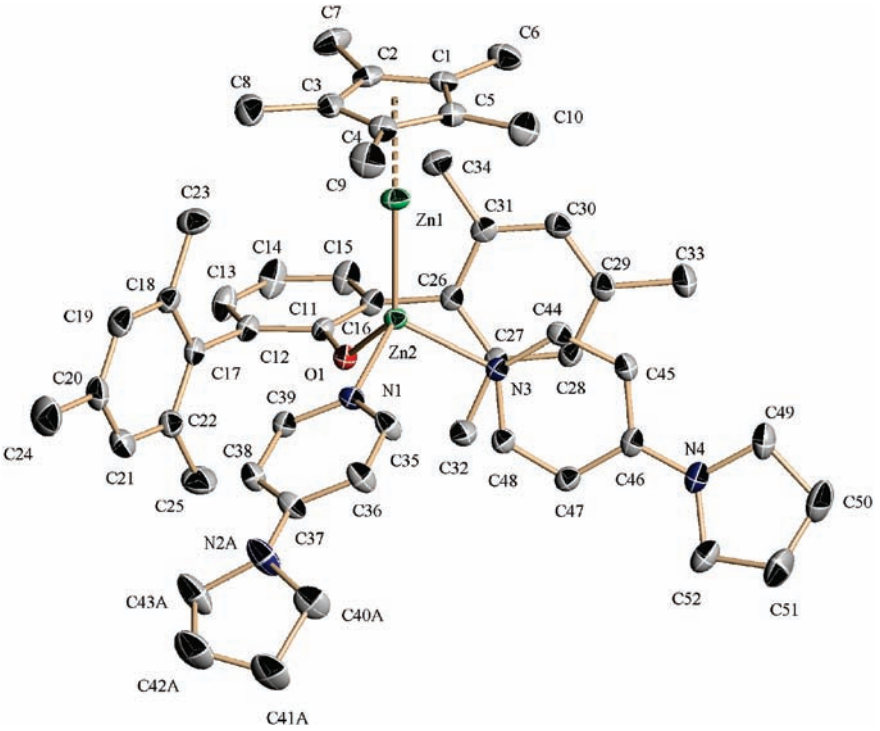

Figure 3. ORTEP view for **7** (displacement ellipsoids are drawn at the 30% probability level). One of the two pyr-py ligands was found disordered in two positions A and B (the occupancy factors were fixed to 0.5 for both). Only the disordered moiety "A" is shown (N2A, C40A, C41A, C42A, C43A). Hydrogen atoms have been omitted for clarity.

former is a MO of a_1 symmetry which results from the antibonding combination of the a_1 π-cyclopentadienyl orbital and the s and p_z metal orbitals, while the SOMO of the latter is also a MO of a_1 symmetry with the same combination of s and p_z metal orbitals (see Scheme 2). In view of the well-known topological analogy of CpM and ML_3 fragments,[17] large differences in the nature of the metal−metal bond between $CpZnZnL_3$ species and $[Zn_2(\eta^5\text{-}C_5Me_5)_2]$ are not actually expected.[18]

Compounds $[Zn_2(\eta^5\text{-}C_5H_5)(py)(\mu\text{-}OC_5H_5)]_2$, **6c**, $[Zn_2(\eta^5\text{-}C_5H_5)(OAr')(py)_2]$ (Ar′ = 2,6-$(C_6H_5)_2C_6H_3$), **7c**, and $[Zn_2(\eta^5\text{-}C_5H_5)(DBU)(\mu\text{-}OC_5H_5)]_2$, **8c**, as models for compounds **6**−**8**, respectively, have been analyzed theoretically by using density functional theory (DFT).[19] Geometry optimizations have been carried out starting with the geometries found by X-ray crystallography (with subsequent simplification of the cyclopentadienyl and pyridine ligands), without symmetry restrictions for

dx.doi.org/10.1021/ic200816f |*Inorg. Chem.* 2011, 50, 6361–6371

models **8c** and **7c** and with imposed C_i symmetry for **6c**. We will center the discussion on compounds **6c** and **7c**, for which the computer-optimized structures are shown in Figure 4. The optimized structure of **8c** is shown in Figure S1 (Supporting Information). In general, a good structural agreement with X-ray data has been found. The Zn−Zn bond is close to 2.32 Å, somewhat shorter than experimental values, as found previously in related calculations that replace C_5Me_5 by C_5H_5.[20] A comparison between selected computed structural parameters and those experimentally found is collected in Table S1 (Supporting Information).

With respect to the nature of the Zn−Zn bond, in complex $[Zn_2(\eta^5\text{-}C_5H_5)(OAr')(py)_2]$, **7c**, the HOMO−1 concentrates the Zn−Zn interaction (with 56% of Zn contribution, see Figure 5). This orbital arises in the model compound from the overlap of the SOMO orbitals of the fragments $(\eta^5\text{-}C_5H_5)Zn$ and $Zn(OAr')(py)_2$ depicted in Scheme 2 that have been computed separately (see Figure S2, Supporting Information). The calculation allows an estimation of ca. 73 kcal·mol^{-1} for the Zn−Zn bond energy in **7c**, which is of the same order of magnitude as that previously computed for related compounds (60−70 kcal·mol^{-1}).[19] The nonsymmetric nature of the Zn−Zn bonding interaction is revealed by the different contributions of the two Zn atoms to the HOMO−1 (30% and 26% for $(\eta^5\text{-}C_5H_5)Zn$ and $Zn(OAr')(py)_2$ zinc atoms, respectively) and also by the disparity of their Mulliken charges (0.12 and 0.57 for $(\eta^5\text{-}C_5H_5)Zn$ and $Zn(OAr')(py)_2$ zinc atoms, respectively). Additionally, small differences have also been found in the orbital composition of each fragment, with 74% and 70% of s character for $(\eta^5\text{-}C_5H_5)Zn$ and $Zn(OAr')(py)_2$, respectively. This nonsymmetric Zn−Zn bond does not imply a weaker interaction, as confirmed by the values of the bond energy (73 kcal·mol^{-1}) and the bond order (0.76), comparable to those calculated for the $[Zn_2(\eta^5\text{-}C_5H_5)_2]$ model.

Scheme 2. Singly Occupied HOMOs of Cp′Zn and ZnL_3 Fragments

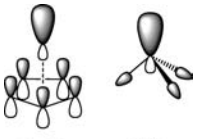

In the tetranuclear complex $[Zn_2(\eta^5\text{-}C_5H_5)(py)(\mu\text{-}OC_5H_5)]_2$, **6c**, the Zn−Zn interaction is quite similar. The two Zn−Zn bonds of this molecule correspond to the HOMO and HOMO−1 (Figure 5) with different Zn contributions to the MOs of 62% and 40%, respectively, but with an identical calculated bond order (0.73). The cyclopentadienyl-bound zinc atom features a higher s orbital preponderance in both MOs (80% and 90% for HOMO and HOMO−1, respectively), in comparison with the pseudo-ZnL_3 fragment (50% and 57% for HOMO and HOMO-1, respectively). Once more, the latter zinc atoms exhibit higher Mulliken charge (0.48) than those bonded to the $\eta^5\text{-}C_5H_5$ ligand (0.24).

Formation of the tetrazinc complex $[Zn_2(\eta^5\text{-}C_5Me_5)(pyr\text{-}py)(\mu\text{-}OC_5Me_5)]_2$, **6**, has been investigated theoretically. Model compound $[Zn_2(\eta^5\text{-}C_5H_5)(OC_5H_5)(py)_2]$, similar to **7c** but with the OC_5H_5 functionality, was optimized without symmetry restrictions (see structure in Figure S3, Supporting Information). The dimerization process to give **6c** plus two molecules of pyridine is exergonic by 24.6 kcal·mol^{-1} at this level of theory. This result supports our proposal that the steric properties of the bulky $Ar^{Mes}O^-$ group stabilizes the monomeric dizinc structure of **7**.[14] The Zn−Zn bond in $[Zn_2(\eta^5\text{-}C_5H_5)(OC_5H_5)(py)_2]$ is analogous to that of **7c** and therefore needs no further discussion (see HOMO and selected data in Supporting Information).

Finally, the hypothetical cation $[(\eta^5\text{-}C_5H_5)ZnZn(py)_3]^+$ has also been optimized with the result that its Zn−Zn bond is similar to that described for **7c** (see Supporting Information). Formation of this species by reaction between the complex $[(\eta^5\text{-}C_5H_5)_2Zn_2]$ and the dication $[Zn_2(py)_6]^{2+}$ is also exergonic (−46.1 kcal·mol^{-1} at this level of theory). Therefore, the synthesis of a complex such as $[(\eta^5\text{-}C_5Me_5)ZnZn(dmap)_3]^+$ can be viewed as a reasonable target.

Electrochemical Studies. Since to our knowledge the electrochemical behavior of $ZnCp^*_2$ and $Zn_2Cp^*_2$ has not yet been described, we searched first for their voltammetric features over an extended potential window (∼ 4 V). Figure 6 illustrates the voltammetric response of a $ZnCp^*_2$ solution starting from a potential of −0.3 V. It can be observed that a wide polarizable window, where no charge transfer takes place, extends from −0.3 to −2.8 V. Upon scanning from −0.3 V toward more negative values (red line scan), a sigmoidal wave A′ develops whose anodic counterpart is the voltammetric peak A centered at −0.6 V. The presence of a hysteresis loop in the cathodic feature together with

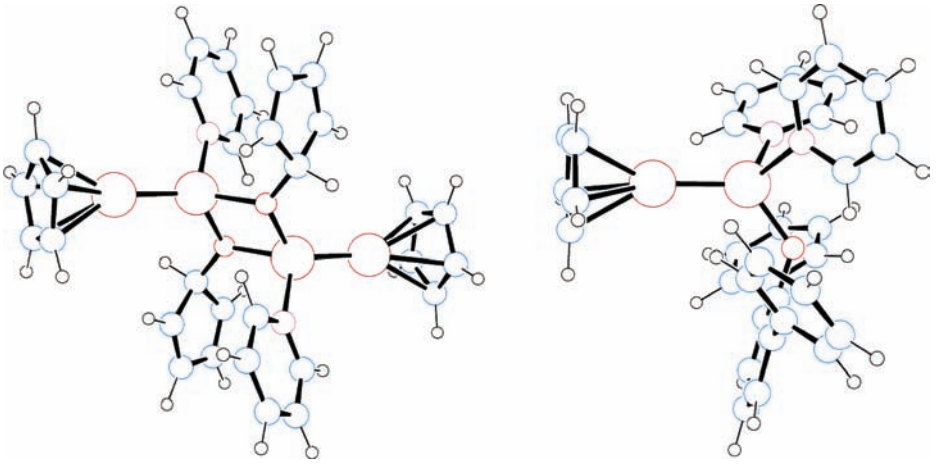

Figure 4. Optimized structures of compounds $[Zn_2(\eta^5\text{-}C_5H_5)(py)(\mu\text{-}OC_5H_5)]_2$, **6c**, and $[Zn_2(\eta^5\text{-}C_5H_5)(OAr')(py)_2]$ (Ar′ = 2,6-$(C_6H_5)_2C_6H_3$), **7c**.

dx.doi.org/10.1021/ic200816f |*Inorg. Chem.* 2011, 50, 6361–6371

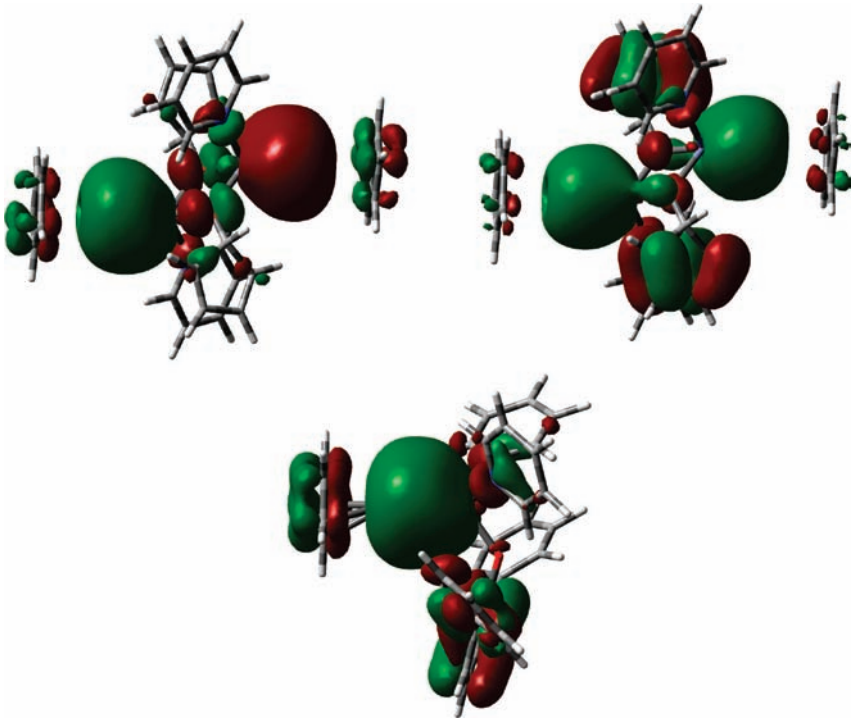

Figure 5. Three-dimensional isosurfaces of the HOMO and HOMO-1 (top) for $[Zn_2(\eta^5\text{-}C_5H_5)(py)(\mu\text{-}OC_5H_5)]_2$, **6c**, and of the HOMO-1 (bottom) for $[Zn_2(\eta^5\text{-}C_5H_5)(OAr')(py)_2]$ (Ar′ = 2,6-$(C_6H_5)_2C_6H_3$), **7c**, which correspond to the Zn−Zn interaction.

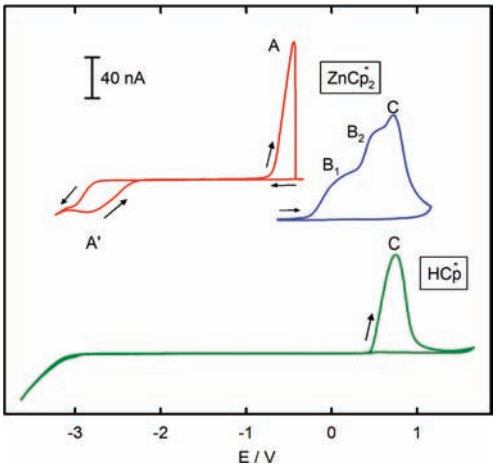

Figure 6. Voltammetric response of a solution containing 20 mM $ZnCp^*_2$, 0.2 M $^tBu_4BF_4$ in THF (red, initial scan toward more negative potentials; blue, initial scan toward more positive potentials) and of a solution containing 10 mM HCp*, 0.2 M $^tBu_4BF_4$ in THF (green). Scan rate: 50 mV/s. For the sake of clarity, voltammograms have been shifted vertically.

the spiked shape of the anodic wave is consistent with formation of a Zn layer on top of the gold surface as the reduction product of $ZnCp^*_2$.

On the other hand, upon scanning the potential toward more positive values than −0.3 V (blue line scan), two plateaus (B1 and B2) and a peak C develop with no cathodic counterpart. The two plateaus are specifically related to oxidation of $ZnCp^*_2$, whereas peak C is also present in the voltammetric fingerprint of HCp* (green line scan) and other metallocenes containing the Cp* ligand. Therefore, peak C is attributed to oxidation of $C_5Me_5^-$ to give the $C_5Me_5^\bullet$ radical, whose dimerization produces dihydrofulvalene, in agreement with previous results of Moulton et al.[21] Then, adsorption of this oxidation product blocks the electrode surface, preventing any further oxidation of $C_5Me_5^-$ and giving rise to a peak-shaped wave. Fortunately, this irreversible oxidation scenario can be easily avoided by setting the anodic scan limit at a potential ≤0.5 V. As illustrated in Figure 7, the two plateaus display now a reversible behavior within the appropriate potential limits. Though not shown, the same overall behavior is observed in the presence of $Zn_2Cp^*_2$ solutions upon scanning the potential between −3 and 1 V.

A closer look at waves B1 and B2 shows that their heights coincide with the expected values for two consecutive monoelectronic oxidation steps. Furthermore, Figure 7 allows their height and location to be compared with those of the well-known Fc^+/Fc couple under the same experimental conditions. It may be observed how both $Zn_2Cp^*_2$ waves appear at potentials slightly more positive (by ca. 30 mV, see Table 1) than those of $ZnCp^*_2$. Besides the close similarities between the two sets of waves, it should be pointed out that the oxidation kinetics of $ZnCp^*_2$ appear to be faster than those of $Zn_2Cp^*_2$, and that the poor definition of the second $Zn_2Cp^*_2$ plateau is likely to be related to a limited stability of the $[Zn_2Cp^*_2]^{2+}$ cation, which would favor an earlier oxidation of the $C_5Me_5^-$ ligand.

Given the lack of detailed information on the electrochemistry of closed shell metallocenes, we also explored the voltammetric behavior of $CaCp^*_2$ and $MgCp^*_2$. A comparison between their voltammetric waves and that of $FeCp^*_2$ is illustrated in Figure 8a. Using the oxidation wave of $FeCp^*_2$ as a reference of a monoelectronic release,[22] the larger height of both $CaCp^*_2$ and $MgCp^*_2$ waves clearly indicates a further change of oxidation

dx.doi.org/10.1021/ic200816f |*Inorg. Chem.* 2011, 50, 6361–6371

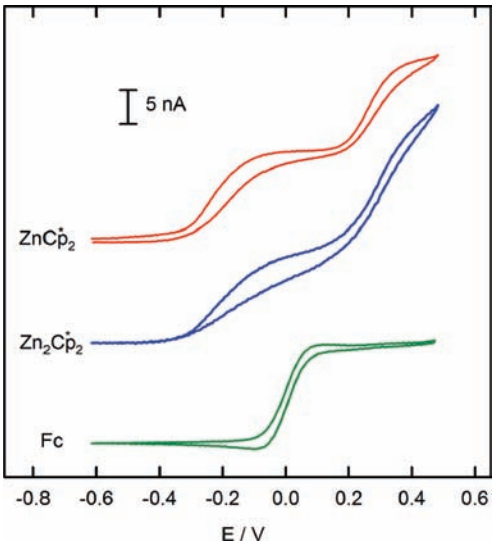

Figure 7. Voltammetric response of 7 mM solutions of $ZnCp^*_2$ (red), $Zn_2Cp^*_2$ (blue), and $FeCp_2$ (green) in 0.2 M $^tBu_4BF_4$ in THF. Scan rate 50 mV/s. For the sake of clarity, voltammograms have been shifted vertically.

Table 1. Half-Wave Potentials of Metallocene Oxidation Waves

	$E_{1/2,1}$/V	$E_{1/2,2}$/V
$FeCp_2$	0.000	
$ZnCp^*_2$	−0.230	0.270
$Zn_2Cp^*_2$	−0.195	0.300
$FeCp^*_2$	−0.445	
$CaCp^*_2$	−0.675	
$MgCp^*_2$	−1.550	−0.435
$Fe(Cp^*Si)_2$	−0.315	
$Mg(Cp^*Si)_2$	−1.445	−0.285
$Mn(Cp^*Si)_2$	−0.835	

state. A single bielectronic wave is observed for $CaCp^*_2$ oxidation, whereas two well-separated waves are recorded in the case of $MgCp^*_2$ oxidation. The $CaCp^*_2$ oxidation wave is located between the two oxidation waves of $MgCp^*_2$, thereby indicating a higher electrochemical stabilization of the $[MgCp^*_2]^+$ cation as compared to $[CaCp^*_2]^+$. It may be worth mentioning that $CaCp^*_2$ and $MgCp^*_2$ differ not only in the size of the metal core but also in their molecular structure.[23] One can then speculate to which point the less solvent-exposed structure of $MgCp^*_2$ may help to stabilize its cationic form. A similar, though much less pronounced, effect becomes evident when comparing the $ZnCp^*_2$ and $Zn_2Cp^*_2$ voltammetric waves.

Another point of interest arises from the different heights of the two $MgCp^*_2$ waves in Figure 8a. The first wave has the same height as the $FeCp^*_2$ wave and can be safely assigned to the $MgCp^*_2 \rightarrow [MgCp^*_2]^+ + e^-$ oxidation. However, the height of the second wave is significantly smaller and also displays some hysteresis; these two characteristics suggest that the $[MgCp^*_2]^+$ cation may be involved in an irreversible following reaction. Though we have not elaborated on the mechanistic details of this hypotetical reaction, we explored the possibility of stabilizing

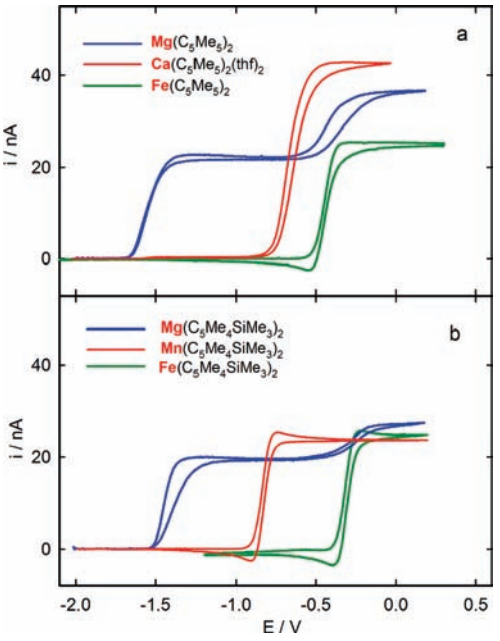

Figure 8. Voltammetric response of 12 mM solutions of (a) $FeCp^*_2$ (green), $CaCp^*_2$ (red), and $MgCp^*_2$ (blue) and (b) $Fe(Cp^*Si)_2$ (green), $Mn(Cp^*Si)_2$ (red), and $Mg(Cp^*Si)_2$ (blue). Scan rate 50 mV/s.

the cation product by using the bulkier ligand $C_5Me_4SiMe_3$ (or Cp*Si in shorthand notation). Figure 8b compares the well-behaved monoelectronic waves of $Mn(Cp^*Si)_2$ and $Fe(Cp^*Si)_2$ with the voltammetric response of $Mg(Cp^*Si)_2$. To our surprise, apart from a systematic shift of ca. 0.1 V in the $E_{1/2}$ value, addition of the new ligand results in a decrease of both plateau currents, so that the presence of deactivating following reactions affects not only to the $[Mg(Cp^*Si)_2]^+$ but also to the neutral $Mg(Cp^*Si)_2$ form.

CONCLUSIONS

The first Zn−Zn-bonded complexes that feature anionic O-containing ligands have been prepared and characterized employing the bulky alcohols C_5Me_5OH and $Ar^{Mes}OH$. The presence of a neutral N donor is additionally required in order to stabilize kinetically the Zn−Zn bond, thwarting disproportionation. In conjunction with pyr-py and DBU, C_5Me_5OH provides dimeric, tetrazinc complexes with two bridging $C_5Me_5O^-$ groups adjoining the dizinc units, whereas the bulkier terphenyloxide $Ar^{Mes}O^-$ gives rise to a dizinc compound with a terminal $Zn-OAr^{Mes}$ bond. Theoretical analysis of $CpZnZnL_3$ compounds confirms the nonsymmetric nature of the Zn−Zn interaction but with practically the same bond energy as symmetric dizinc species. Noteworthy general features are higher charge and lower participation of the s orbital of the zinc atom within the ZnL_3 fragment with respect to the metal that forms the CpZn unit. Two monoelectronic oxidation steps have been found by cyclic voltammetry for $[Zn_2(\eta^5\text{-}C_5Me_5)_2]$ as well as for the close-shell metallocenes $M(C_5Me_5)_2$ for M = Zn, Mg, Ca. These steps may appear as two well-resolved waves, as in the case of $ZnCp^*_2$, $Zn_2Cp^*_2$, $MgCp^*_2$, and $Mg(Cp^*Si)_2$, or they can merge in a single bielectronic wave, as in the case of $CaCp^*_2$. Moreover, the oxidation products of $MgCp^*_2$ and $Mg(Cp^*Si)_2$

dx.doi.org/10.1021/ic200816f |Inorg. Chem. 2011, 50, 6361–6371

undergo further chemical reactions, resulting in a significant lowering of the diffusion-limiting plateau currents.

EXPERIMENTAL SECTION

General Considerations. All preparations and manipulations were carried out under oxygen-free argon using conventional Schlenk techniques, in most cases at low temperatures. Compounds **5, 6**, **7**, and **8** have to be stored under nitrogen at −20 °C to avoid decomposition. Solvents were rigorously dried and degassed before use. Solution NMR spectra were recorded on Bruker AMX-300, DRX-400, and DRX-500 spectrometers. The ^{1}H and ^{13}C resonances of the solvent were used as the internal standard, and the chemical shifts are reported relative to TMS. FAB-MS analyses were carried out in a Waters AUOSPEC-Q spectrometer using 3-nitrobenzyl alcohol as the matrix. Yields of the metal complexes are based on zinc. $[Zn_2(\eta^5\text{-}C_5Me_5)_2]$,[7b] C_5Me_5OH,[24] and $Ar^{Mes}OH$[25] were prepared according to literature methods. Other chemicals were commercially available and used as received. The thermal instability and extreme reactivity of compounds **5**−**8** toward oxygen and water do not allow performing elemental analyses and high-resolution mass spectrometry.

Synthesis of $[(\eta^5\text{-}C_5Me_5)Zn\{2,6\text{-}(2,6\text{-}^{i}Pr_2C_6H_3)_2\text{-}C_6H_3\}]$ (2). $\{2,6\text{-}(2,6\text{-}^{i}Pr_2C_6H_3)_2\text{-}C_6H_3\}Li$ (1.55 g, 3.83 mmol) and $ZnCp^*_2$ (1.29 g, 3.84 mmol) were mixed in Et_2O (30 mL). A colorless suspension formed, which was stirred for 20 h at room temperature. After removing the solid (LiCp*) by filtration, the solvent was evaporated under reduced pressure. The colorless oily residue was extracted with pentane (10 mL) and filtered. After addition of ca. 0.5 mL of benzene, the resulting solution was put in the fridge at −20 °C and a crystalline solid separated out. The mother liquor was transferred into another flask and dried *under vacuum* to give a colorless solid identified as **2** (1.25 g, 2.09 mmol, 55%). ^{1}H NMR (400.13 MHz): δ 7.28 and 7.20 (AB_2 spin system, 6H, $^{3}J_{HH}$ = 7.80 Hz, aryl protons of $C_6H_3{}^{i}Pr_2$), 7.13 and 7.07 (AB_2 spin system, 3H, $^{3}J_{HH}$ = 8.8 Hz, aryl protons of $C_6H_3Ar_2$), 2.90 (sept, 4H, $^{3}J_{HH}$ = 6.9 Hz, $CHCH_3$), 1.64 (s, 15H, CH_3 of Cp*), 1.27 (d, 12H, $^{3}J_{HH}$ = 6.9 Hz, $CHCH_3$), 1.05 (d, 12H, $^{3}J_{HH}$ = 6.9 Hz, $CHCH_3$) ppm. $^{13}C\{^{1}H\}$ NMR (100.67 MHz): 150.2 (s, *ortho* of $C_6H_3Ar_2$), 149.2 (s, *ipso* of $C_6H_3Ar_2$), 146.3 (s, *ortho* of $C_6H_3{}^{i}Pr_2$), 145.9 (s, *ipso* of $C_6H_3{}^{i}Pr_2$), 127.9 (s, *para* of $C_6H_3{}^{i}Pr_2$), 127.1 (s, *para* of $C_6H_3Ar_2$), 126.2 (s, *meta* of $C_6H_3Ar_2$), 123.4 (s, *meta* of $C_6H_3{}^{i}Pr_2$), 109.0 (s, CCH_3 of Cp*), 30.6 (s, $CHCH_3$), 25.2 (s, $CHCH_3$), 23.4 (s, $CHCH_3$), 10.7 (s, CH_3 of Cp*) ppm. FAB MS: *m*/*z* calcd for $C_{40}H_{52}Zn$ 596.3360; found 596.3387.

Synthesis of $[(\eta_5\text{-}C_5Me_5)Zn\{2,6\text{-}(2,6\text{-}Me_2C_6H_3)_2\text{-}C_6H_3\}]$ (3). The compound was prepared similarly to **2** using $\{2,6\text{-}(2,6\text{-}Me_2C_6H_3)_2\text{-}C_6H_3\}Li$ instead of $\{2,6\text{-}(2,6\text{-}^{i}Pr_2C_6H_3)_2\text{-}C_6H_3\}Li$. Yield: 1.30 g, 2.69 mmol, 66%. ^{1}H NMR (400.13 MHz, C_6D_6): δ 6.80−7.20 (m, 9H, aromatic protons), 2.02 (s, 12H, CH_3 of $C_6H_3Me_2$), 1.62 (s, 15H, CH_3 of Cp*) ppm. $^{13}C\{^{1}H\}$ NMR (100.63 MHz, C_6D_6): 151.3 (s, *ortho* of $C_6H_3Ar_2$), 147.4 (s, *ipso* of $C_6H_3Me_2$), 146.2 (s, *ipso* of $C_6H_3Ar_2$), 135.8 (s, *ortho* of $C_6H_3Me_2$), 128.5 (s, *para* of $C_6H_3Ar_2$), 128.1 (s, *meta* of $C_6H_3Me_2$), 127.1 (para of $C_6H_3Me_2$), 125.4 (s, *meta* of $C_6H_3Ar_2$), 107.8 (s, CCH_3 of Cp*), 20.9 (s, CH_3 of $C_6H_3Me_2$), 9.6 (s, CH_3 of Cp*). FAB MS: *m*/*z* calcd for $C_{32}H_{36}Zn$ 484.2118; found 484.2108.

Synthesis of $[Zn_2Cp^*_2(DBU)_2]$ (4). The compound was prepared by addition of 2 equiv of pure DBU to 30 mg of $Zn_2Cp^*_2$ dissolved in approximately 0.5 mL of C_6D_6 and characterized in situ. ^{1}H NMR (400.13 MHz, C_6D_6): 3.12 (m, 4H; H4), 2.58−2.52 and 2.30−2.27 (m, 12H; H2, H6, H10), 2.21 (s, 30H, CH_3), 1.48−1.42, 1.40−1.34, 1.27−1.21 and 1.10−1.04 (m, 16H; H3, H7, H8, H9) ppm. $^{13}C\{^{1}H\}$ NMR (100.63 MHz): 161.0 (s, C═N), 109.6 (s, CCH_3), 52.5 (s, NCH_2), 48.1 (s, NCH_2), 43.8 (s, NCH_2), 37.0 (s, CH_2), 29.7 (s, CH_2), 28.4 (s, CH_2), 26.1 (s, CH_2), 22.8(s, CH_2), 11.4 (s, CH_3 of Cp*) ppm.

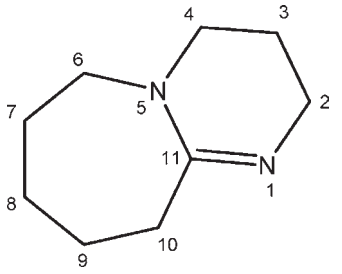

Synthesis of $[Zn_2Cp^*_2(pyr\text{-}py)_2]$ (5). A solution of 4-pyrrolidinopyridine in Et_2O (120 mg, 0.81 mmol in 10 mL) was added slowly to a solution of $Zn_2Cp^*_2$ in Et_2O (150 mg, 0.372 mmol in 10 mL) at −10 °C. A yellow solution was obtained which was allowed to reach room temperature and stirred for 30 min. The solution was concentrated to ca. 3 mL by evaporation of the solvent under reduced pressure, and pentane was added at −20 °C. The resulting suspension was filtered, and the yellow air-sensitive solid was collected by filtration, washed with pentane (5 mL), and dried quickly *under vacuum*. Yield: 240 mg, 93%. ^{1}H NMR (300.13 MHz, C_6D_6, 279 K): 8.43 (d, 4H, $^{3}J_{HH}$ = 5.0 Hz, pyr^2), 6.06 (d, 4H, $^{3}J_{HH}$ = 5.0 Hz, pyr^3), 2.63−2.59 (m, 8H, NCH_2), 2.06 (s, 30H, CH_3 of Cp*), 1.31−1.26 (m, 8H, NCH_2CH_2) ppm. $^{13}C\{^{1}H\}$ NMR (125.78 MHz): 151.7 (s, pyr^4), 150.1 (s, pyr^2), 109.5 (s, CCH_3), 107.1 (s, pyr^3), 46.5 (s, NCH_2CH_2), 25.1 (s, NCH_2CH_2), 10.9 (s, CH_3 of Cp*) ppm.

Synthesis of $[Zn_2Cp^*(pyr\text{-}py)(OCp^*)]_2$ (6). A solution of 4-pyrrolidinopyridine in toluene (196 mg, 1.32 mmol in 10 mL) was added slowly to a solution of $Zn_2Cp^*_2$ in toluene (250 mg, 0.62 mmol in 10 mL) at −10 °C. The solution quickly turned yellow. At −25 °C, an ether solution of Cp*OH was carefully layered on the yellow toluene of **4** and the Schlenk tube was then put in the fridge at −20 °C. Colorless crystals of **6** formed and were isolated, washed with pentane, and dried in vacuo. Yield: 280 mg (80%). ^{1}H NMR (500.13 MHz, toluene-d_8): δ 8.43 (d, 4H, $^{3}J_{HH}$ = 5.0 Hz, pyr^2), 6.06 (d, 4H, $^{3}J_{HH}$ = 5.0 Hz, pyr^3), 2.63−2.59 (m, 8H, NCH_2), 2.41 (s, 30H, CH_3 of C_5Me_5), 1.99 (s, 12H, β CH_3 of OC_5Me_5), 1.67 (s, 12H, γ CH_3 of OC_5Me_5), 1.36−1.31 (m, 8H, NCH_2CH_2), 1.20 (s, 6H, α CH_3 of OC_5Me_5) ppm. $^{13}C\{^{1}H\}$ NMR (125.78 MHz, toluene-d_8, 223 K): δ 149.7 (s, py^2), 140.2 (s, β CCH3 of OC_5Me_5), 127.5 (s, γ CCH3 of OC_5Me_5), 107.8 (s, CCH_3 of OC_5Me_5), 106.7 (s, py^3), 85.6 (s, α CCH_3 of OC_5Me_5), 45.9 (s, NCH_2), 24.8 (s, NCH_2CH_2), 21.4 (s, α CH_3 of OC_5Me_5), 11.4 (s, β or γ CH_3 of OC_5Me_5), 10.9 (s, CH_3 of C_5Me_5), 9.1 (s, β or γ CH_3 of OC_5Me_5) ppm (py^4 not observed).

Synthesis of $[Zn_2Cp^*(pyr\text{-}py)_2(OAr^{Mes})]$ (7). The compound was prepared and crystallized similarly to **6** using $Ar^{Mes}OH$ instead of Cp*OH. Yield: 160 mg (80%). ^{1}H NMR (300.13 MHz, C_6D_6): 7.83 (d, 4H, $^{3}J_{HH}$ = 6.1 Hz, pyr^2), 7.26 (d, $^{3}J_{HH}$ = 7.3 Hz, *meta* H of $C_6H_3Ar_2$), 6.95 (t, $^{3}J_{HH}$ = 7.3 Hz, *para* H of $C_6H_3Ar_2$), 6.84 (s, 4H, *meta* H of $C_6H_2Me_3$), 5.85 (d, 4H, $^{3}J_{HH}$ = 6.1 Hz, pyr^3), 2.54 (s, 15H, CH_3 of Cp*), 2.54−2.48 (m, 8H, NCH_2), 2.38 (s, 12H, *ortho* CH_3), 2.27 (s, 6H, *para* CH_3), 1.26−1.17 (m, 8H, NCH_2CH_2) ppm. $^{13}C\{^{1}H\}$ NMR (125.78 MHz, THF-d_8, 263 K): 164.5 (s, C-OZn), 152.8 (s, py^4), 148.8 (s, py^2), 147.1 (s, *ipso* of $C_6H_2Me_3$) 141.1 (s, *ortho* C of $C_6H_3Ar_2$), 137.8 (s, *ortho* CCH_3 of $C_6H_2Me_3$), 134.5 (s, *para* CCH_3 of $C_6H_2Me_3$), 132.2 (s, *meta* CH of $C_6H_2Ar_2$), 129.2 (s, *para* CH of $C_6H_2Ar_2$), 128.2 (s, *meta* CCH_3 of $C_6H_2Me_3$), 108.4 (s, CCH_3 of Cp*), 107.0 (s, py^3), 47.8 (s, NCH_2), 26.3 (s, NCH_2CH_2), 22.0 (s, *ortho* CH_3 of $C_6H_2Me_3$), 21.7 (s, *para* CH_3 of $C_6H_2Me_3$), 11.3 (s, CH_3 of Cp*).

Synthesis of $[Zn_2(\eta^5\text{-}C_5Me_5)(DBU)(\mu\text{-}OC_5Me_5)]_2$ (8). The compound was prepared and crystallized similarly to **6** using DBU instead of pyr-py. Yield: 180 mg (85%). ^{1}H NMR (300.13 MHz, C_6D_6):

Table 2. Crystal Data for $2\cdot 0.5(C_6H_6)$, 6, $7\cdot Et_2O\cdot C_7H_8$, and 8[a]

	2	6	7	8
empirical formula	$C_{40}H_{52}Zn\ 0.5(C_6H_6)$	$C_{72}H_{100}N_4O_2Zn_4$	$C_{52}H_{64}N_4OZn_2\cdot C_4H_{10}O\cdot C_7H_8$	$C_{29}H_{46}N_2OZn_2$
fw	637.24	1315.04	1058.07	569.42
temp./K	173(2)	173(2)	173(2)	100(2)
cryst syst	monoclinic	triclinic	monoclinic	monoclinic
space group	$P2_1/n$	P_T	$C2/c$	$P2_1/n$
a/Å	10.7913(8)	12.1601(17)	29.4692(7)	9.1353(8)
b/Å	15.3326(13)	12.9369(18)	14.0062(3)	22.0335(14)
c/Å	22.3159(16)	13.6190(19)	31.3110(7)	14.2988(12)
α/deg	90	103.123(5)	90	90
β/deg	95.310(2)	109.060(5)	115.1140(10)	91.452(4)
γ/deg	90	110.926(5)	90	90
vol./Å^3	3676.5(5)	1742.2(4)	11701.9(5)	2877.2(4)
Z	4	1	8	4
D_{calcd}/g cm^{-3}	1.151	1.253	1.201	1.315
$F(000)$	1372	696	4512	1208
cryst size (mm^3)	0.24 × 0.24 × 0.13	0.36 × 0.21 × 0.20	0.50 × 0.45 × 0.14	0.25 × 0.21 × 0.16
θ range/deg	1.61 to 30.52.	1.72 to 30.78	1.44 to 30.56	1.70 to 27.12
index ranges	$-15 \le h \le 10$	$-17 \le h \le 17$	$-42 \le h \le 30$	$-10 \le h \le 11$,
	$-21 \le k \le 21$	$-18 \le k \le 11$	$-20 \le k \le 20$	$-25 \le k \le 28$,
	$-30 \le l \le 31$	$-19 \le l \le 19$	$-24 \le l \le 44$	$-15 \le l \le 18$
reflns collected	46 824	37 936	122 515	17 316
independent reflns	10 825[R(int) = 0.0622]	10 557[R(int) = 0.0720]	17 463[R(int) = 0.0489]	6348 [R(int) = 0.0667]
data/restraints/parameters	10 825/0/410	10 557/0/381	17 463/0/712	6348/0/317
goodness-of-fit on F^2	1.040	1028	1.060	1.027
Final R indices [$I > 2\sigma(I)$]	R1 = 0.0514, wR2 = 0.1197	R1 = 0.0599, wR2 = 0.1341	R1 = 0.0541, wR2 = 0.1249	R1 = 0.0522, wR2 = 0.1356
R indices (all data)	R1 = 0.0958, wR2 = 0.1395	R1 = 0.0901, wR2 = 0.2182	R1 = 0.0860, wR2 = 0.1424	R1 = 0.0771, wR2 = 0.1510

[a] Absorption correction: semi-empirical from equivalent. Refinement method: full-matrix least-squares on F2. Wavelength = 0.71073 Å.

δ 3.41 (t, 4H, $^3J_{HH}$ = 5.3 Hz; H4), 2.66−2.54 (m, 12H; H10, H6, and H2), 2.26 (s, 30H, CH_3 of C_5Me_5), 1.98 (s, 12H, β CH_3 of OC_5Me_5), 1.79 (s, 12H, γ CH_3 of OC_5Me_5), 1.58−1.42 (m, 8H; H9 and H3), 1.34−1.24 (m, 4H; H8), 1.33 (s, 6H, α CH_3 of OC_5Me_5), 1.13−1.03 (m, 4H; H7) ppm.

Computational Details. The electronic structure and geometries of compounds **6c**−**8c** were computed by density functional theory at the B3LYP level.[26] The atoms were described using the 6-31G** basis set. The optimized geometries of all compounds were characterized as energy minima either by the absence of imaginary frequencies (NImag = 0) or by very low vibrational frequencies (<25 cm^{-1}) in the diagonalization of the analytically computed Hessian (vibrational frequencies calculations). These very low vibrational frequencies that do not lead to energy minimum optimization have been reported in other cases and seem to be associated to numerical errors in the DFT integration grid. They could be eliminated by much more expensive calculation with a better grid.[27] MO analysis of $(\eta^5\text{-}C_5H_5)Zn$ and $Zn(OAr')(py)_2$ (Ar′ = 2,6-$(C_6H_5)_2C_6H_3$) metal fragments of 7**c** was carried out by computing them at the same level of theory with the frozen geometries found in the optimized complex. The bond energy of the Zn−Zn bond was calculated directly by subtracting the energies of the optimized binuclear complex and the two mononuclear fragments that have the geometry they adopt in the complex. Composition of MOs and bond orders were obtained using the Chemissian program.[28] DFT calculations were performed using the Gaussian 03 suite of programs.[29] Cartesian coordinates of the optimized compounds are collected in the Supporting Information (Table 2).

Electrochemical Measurements. Electrochemical measurements were carried out in a three-electrode glass cell, thermostated at −15 ± 0.2 °C with a Haake D8.G circulator thermostat. Cell and electrodes were kept inside a glovebox under nitrogen overpressure. Working solutions were prepared in the electrochemical cell by dissolving weighted amounts of $^tBu_4BF_4$ and the metallocene of interest in 4 cm^3 of freshly distilled THF. Transfer of the solution components to the glovebox was performed under inert atmosphere conditions. A Ag/AgCl wire immersed in a 0.2 M $^tBu_4BF_4$ THF solution and a gold wire were used as reference and auxiliary electrodes, respectively. The working ultramicroelectrode was a polycrystalline gold disk of 25 μm diameter, whose surface was polished with 0.05 μm alumina powder (Buheler). At the end of each run of experiments a given amount of $FeCp_2$ was added to the solution and the $FeCp_2^+/FeCp_2$ half-wave potential $E_{1/2}^{Fc^+/Fc}$ was determined from its voltammetric response. All potential values were then referred to the ferrocenium/ferrocene potential scale by subtracting $E_{1/2}^{Fc^+/Fc}$ from the experimentally recorded potentials.[30] Voltammetric measurements were carried out with an Autolab PGSTAT30 (Eco Chemie).

X-ray Structural Characterization of 2. Crystals suitable for X-ray diffraction were grown from pentane/benzene at −20 °C (vide supra). A single crystal of suitable size, coated with dry perfluoropolyether, was mounted on a glass fiber and fixed in a cold nitrogen stream [T = 173(2) K] to the goniometer head. Data collection was performed on Bruker-Nonius X8APEX-II CCD diffractometer, using monochromatic radiation λ(Mo $K_{\alpha 1}$) = 0.71073 Å, by means of ω and φ scans. The data were reduced (SAINT)[31] and corrected for Lorentz polarization effects and absorption by multiscan method applied by SADABS.[32]

dx.doi.org/10.1021/ic200816f |Inorg. Chem. 2011, 50, 6361–6371

The structure was solved by direct methods (SIR-2002)[33] and refined against all F^2 data by full-matrix least-squares techniques (SHELXTL-6.12).[34] All non-hydrogen atoms were refined with anisotropic displacement parameters. The hydrogen atoms were included from calculated positions and refined riding on their respective carbon atoms with isotropic displacement parameters. Details are given in Table 2. CCDC nos. 828096, 773522, 773521, 773523, and 828097 contains the supplementary crystallographic data for this paper. These data can be obtained free of charge from The Cambridge Crystallographic Data Centre via www.ccdc.cam.ac.uk/data_request/cif.

■ ASSOCIATED CONTENT

Supporting Information. Chemical reactivity DFT calculations and electrochemistry of metal−metal-bonded zincocenes. This material is available free of charge via the Internet at http://pubs.acs.org.

■ AUTHOR INFORMATION

Corresponding Author
*Fax: (+) 34-954460565. E-mail: guzman@us.es.

■ ACKNOWLEDGMENT

Financial support (FEDER contribution and Subprograma Juan de la Cierva) from the Spanish Ministry of Science and Innovation (Projects CTQ2010-15833 and Consolider-Ingenio 2010 CSD2007-00006) and the Junta de Andalucía (Grant FQM-119 and Project P09-FQM-5117) is gratefully acknowledged. M.C. thanks the Spanish Ministry of Education for a research grant (AP-4193). J.J.C. and R.A. acknowledge financial support from the DGICYT under grant CTQ 2008-00371 and from the Junta de Andalucía under grant P07-FQM-02492. A.G. thanks the MICINN (Project CTQ2010-15515) and Junta de Andalucía (Proyecto de Excelencia, FQM-02474) for their financial support for this research. We are grateful to CICA and UGRGrid (Universidad de Granada) for permitting the use of their computational resources.

■ DEDICATION

In memoriam of Professor Rafael Suau, a dear friend and reputed colleague.

■ REFERENCES

(1) (a) Kealy, T. J.; Pauson, P L. *Nature* **1951**, *168*, 1039. (b) Miller, S. A.; Tebboth, J. A.; Tremaine, J. F. *J. Chem. Soc.* **1952**, 633. (c) Fischer, E. O.; Pfab, W. *Z. Naturforsch.* **1952**, *7b*, 377. (d) Wilkinson, G.; Rosenblum, M; Whiting, M. C.; Woodward, R. B. *J. Am. Chem. Soc.* **1952**, *74*, 2125. (e) Wilkinson, G. *J. Am. Chem. Soc.* **1952**, *74*, 6146.

(2) (a) Jutzi, P.; Burdford, N. In *Metallocenes*; Togni, A., Halterman, R. L., Eds.; Wiley-VHC: Weinheim, Germany, 1998; Vol. 1, Chapter 1; (b) In *Metallocene-Based Polyolefins*; Scheirs, J., Kaminsky, W., Eds.; John Wiley & Sons Ltd.: Chichester, 2000; Vols. 1 and 2. (c) *Ferrocenes*; Togni, A., Hayashi, T., Eds.; Verlach Chemie: Weinheim, Germany, 1995.

(3) (a) Arndtsen, B. A.; Bergman, R. G. *Science* **1995**, *270*, 1970. (b) Chen, H.; Schlecht, S.; Semple, T. C.; Hartwig, J. F. *Science* **2000**, *287*, 1995. (c) Pamplin, C. B.; Legzdins, P. *Acc. Chem. Res.* **2003**, *36*, 223. (d) Jones, W. D. *Inorg. Chem.* **2005**, *44*, 4475. (e) Jaouen, G.; Top, S.; Vessières, A.; Alberto, R. *J. Organomet. Chem.* **2000**, *600*, 23.

(4) (a) Jutzi, P.; Burford, N. *Chem. Rev.* **1999**, *99*, 969. (b) Janiak, C.; Schumann, H. *Adv. Organomet. Chem.* **1991**, *23*, 291. (c) Hays, M. L.; Hanusa, T. P. *Adv. Organomet. Chem.* **1996**, *40*, 117.

(5) (a) Blom, R.; Boersma, J.; Budzelaar, P. H. M.; Fischer, B.; Haaland, A.; Volden, H. V.; Weidlein, J. *Acta Chem. Scand.* **1986**, *A40*, 113. (b) Fischer, B.; Wijkens, P.; Boersma, J.; van Koten, G.; Smeets, W. J. J.; Spek, A. L.; Budzelaar, P. H. M. *J. Organomet. Chem.* **1989**, *376*, 223. (c) Burkey, D. J.; Hanusa, T. P. *J. Organomet. Chem.* **1996**, *512*, 165.

(6) (a) Fischer, E. O.; Hofmann, H. P.; Treiber, A. *Z. Naturforsch. B* **1959**, *14*, 599. (b) Ly, H. V.; Forster, T. D.; Parvez, M.; McDonald, R.; Roesler, R. *Organometallics* **2007**, *26*, 3516. (c) Ly, H. V.; Forster, T. D.; Maley, D.; Parvez, M.; Roesler, R. *Chem. Commun.* **2005**, 4468. (d) Budzelaar, P. H. M.; Boersma, J.; van der Kerk, G. J. M.; Spek, A. L.; Duisenberg, A. J. M. *J. Organomet. Chem.* **1985**, *281*, 123. (e) Álvarez, E.; Grirrane, A.; Resa, I.; del Río, D.; Rodríguez, A.; Carmona, E. *Angew. Chem., Int. Ed.* **2007**, *46*, 1296.

(7) (a) Resa, I.; Carmona, E.; Gutiérrez Puebla, E.; Monge, A. *Science* **2004**, *305*, 1136. (b) Grirrane, A.; Resa, I.; Rodríguez, A.; Carmona, E.; Álvarez, E.; Gutiérrez Puebla, E.; Monge, A.; Galindo, A.; del Río, D.; Andersen, R. H. *J. Am. Chem. Soc.* **2007**, *129*, 693.

(8) (a) Zhu, Z.; Wright, R. J.; Olmstead, M. M.; Rivard, E.; Brynda, M.; Power, P. P. *Angew. Chem., Int. Ed.* **2006**, *45*, 5807. (b) Zhu, Z.; Brynda, M.; Wright, R. J.; Fischer, R. C.; Merrill, W. A.; Rivard, E.; Wolf, R.; Fettinger, J. C.; Olmstead, M. M.; Power, P. P. *J. Am. Chem. Soc.* **2007**, *129*, 10847. (c) Zhu, Z.; Fettinger, J. C.; Olmstead, M. M.; Power, P. P. *Organometallics* **2009**, *28*, 1590. (d) Carmona, E.; Galindo, A. *Angew. Chem., Int. Ed.* **2008**, *47*, 6526.

(9) (a) Wang, Y.; Quillian, B.; Wei, P.; Wang, H.; Yang, X.-J.; Xie, Y.; King, R. B.; Schleyer, P. v. R.; Schaefer, H. F., III; Robinson, G. H. *J. Am. Chem. Soc.* **2005**, *127*, 11944. (b) Fedushkin, I. L.; Skatova, A. A.; Ketkov, S. Y.; Eremenko, O. V.; Piskunov, A. V.; Fukin, G. K. *Angew. Chem., Int. Ed.* **2007**, *46*, 4302. (c) Fedushkin, I. L.; Eremenko, O. V.; Skatova, A. A.; Piskunov, A. V.; Fukin, G. K.; Ketkov, S. Y. *Organometallics* **2009**, *28*, 3863. (d) Bollermann, T.; Freitag, K.; Gemel, C.; Seidel, R. W.; von Hopffgarten, M.; Frenking, G.; Fischer, R. A. *Angew. Chem., Int. Ed.* **2010**, *50*, 772.

(10) (a) Yang, X.-J.; Yu, J.; Liu, Y.; Xie, Y.; Schaefer, H. F., III; Liang, Y.; Wu, B. *Chem. Commun.* **2007**, 2363. (b) Tsai, Y.-C.; Lu, D.-Y.; Lin, Y.-M.; Hwang, J.-K.; Yub, J.-S. K. *Chem. Commun.* **2007**, 4125. (c) Yu, J.; Yang, X.-J.; Liu, Y.; Pu, Z.; Li, Q.-S.; Xie, Y.; Schaefer, H. F.; Wu, B. *Organometallics* **2008**, *27*, 5800.

(11) (a) Green, S. P.; Jones, C.; Stasch, A. *Science* **2007**, *318*, 1754. (b) Green, S. P.; Jones, C.; Stasch, A. *Angew. Chem., Int. Ed.* **2008**, *47*, 9079. (c) Liu, Y.; Li, S.; Yang, X.-J.; Yang, P.; Wu, B. *J. Am. Chem. Soc.* **2009**, *131*, 4210. (d) Bonyhady, J. S.; Jones, C.; Nembenna, S.; Stasch, A.; Edwards, A. J.; McIntyre, G. J. *Chem.—Eur. J.* **2010**, *16*, 938.

(12) (a) Schuchmann, D.; Westphal, U.; Schulz, S.; Flörke, U.; Bläser, D.; Boese, R. *Angew. Chem., Int. Ed.* **2009**, *48*, 807. (b) Schulz, S.; Schuchmann, D.; Krossing, I.; Himmel, D.; Bläser, D.; Boese, R. *Angew. Chem., Int. Ed.* **2009**, *48*, 5748.

(13) (a) Schulz, S.; Schuchmann, D.; Westphal, U.; Bolte, M. *Organometallics* **2009**, *28*, 1590. (b) Schulz, S.; Gondzik, S.; Schuchmann, D.; Westphal, U.; Dobrzycki, L.; Boese, R.; Harder, S. *Chem. Commun.* **2010**, *46*, 7757. (c) Gondzik, S.; Bläser, D.; Wölper, C.; Schulz, S. *Chem.—Eur. J.* **2010**, *16*, 13599. (d) Nayek, H. P.; Lühl, A.; Schulz, S.; Köppe, R.; Roesky, P. W. *Chem.—Eur. J.* **2011**, *17*, 1773.

(14) Carrasco, M.; Peloso, R.; Rodríguez, A.; Álvarez, E.; Maya, C.; Carmona, E. *Chem.—Eur. J.* **2010**, *16*, 9754.

(15) Resa, I.; Álvarez, E.; Carmona, E. *Z. Anorg. Allg. Chem.* **2007**, *633*, 1827.

(16) Kaljurand, I.; Kütt, A.; Sooväli, L.; Rodima, T.; Mäemets, V.; Leito, I.; Koppel, I. A. *J. Org. Chem.* **2005**, *70*, 1019.

(17) (a) Albright, T. A.; Burdett, J. K.; Whangbo, M.-H. *Orbital interactions in chemistry*; Wiley: New York, 1985. (b) Jean, Y. *Molecular orbitals of transition metal complexes*; Oxford University Press: New York, 2005.

(18) Neutral compounds of general formula L_3ZnZnL_3 are unknown, but DFT calculations of these complexes anticipate their stability. Galindo, A. Unpublished results.
(19) Parr, R. G.; Yang, W. *Density Functional Theory of Atoms and Molecules*; Oxford University Press: New York, 1989.
(20) del Río, D.; Galindo, A.; Resa, I.; Carmona, E. *Angew. Chem., Int. Ed.* **2005**, *44* (8), 1244.
(21) Moulton, R. D.; Farid, R.; Bard, A. J. *J. Electroanal. Chem.* **1988**, *256*, 309.
(22) Noviandri, I.; Brown, K. N.; Fleming, D. S.; Gulyas, P. T.; Lay, P. A.; Masters, A. F.; Phillips, L. *J. Phys. Chem. B* **1999**, *103*, 6713.
(23) Rayón, V. M.; Frenking, G. *Chem.—Eur. J.* **2002**, *8*, 4693.
(24) Macaulay, J. B.; Fallis, A. G. *J. Am. Chem. Soc.* **1990**, *112*, 1136.
(25) Stanciu, C.; Olmstead, M. M.; Phillips, A. D.; Stender, M.; Power, P. P. *Eur. J. Inorg. Chem.* **2003**, 3495.
(26) (a) Lee, C.; Yang, W.; Parr, R. G. *Phys. Rev. B* **1988**, *37*, 785. (b) Becke, A. D. *J. Chem. Phys.* **1993**, *98*, 5648.
(27) See, for example: (a) Lignell, A.; Khriachtchev, L.; Räsänen, M.; Pettersson, M. *Chem. Phys. Lett.* **2004**, *390*, 256. (b) van Slageren, J.; Klein, A.; Zalis, S.; Stufkens, D. J. *Coord. Chem. Rev.* **2001**, *219−221*, 937.
(28) Leonid, S. *Chemissian 1.771*; 2005−2010. http://www.chemissian.com
(29) Frisch, M. J.; Trucks, G. W.; Schlegel, H. B.; Scuseria, G. E.; Robb, M. A.; Cheeseman, J. R.; Montgomery, Jr., J. A.; Vreven, T.; Kudin, K. N.; Burant, J. C.; Millam, J. M.; Iyengar, S. S.; Tomasi, J.; Barone, V.; Mennucci, B.; Cossi, M.; Scalmani, G.; Rega, N.; Petersson, G. A.; Nakatsuji, H.; Hada, M.; Ehara, M.; Toyota, K.; Fukuda, R.; Hasegawa, J.; Ishida, M.; Nakajima, T.; Honda, Y.; Kitao, O.; Nakai, H.; Klene, M.; Li, X.; Knox, J. E.; Hratchian, H. P.; Cross, J. B.; Bakken, V.; Adamo, C.; Jaramillo, J.; Gomperts, R.; Stratmann, R. E.; Yazyev, O.; Austin, A. J.; Cammi, R.; Pomelli, C.; Ochterski, J. W.; Ayala, P. Y.; Morokuma, K.; Voth, G. A.; Salvador, P.; Dannenberg, J. J.; Zakrzewski, V. G.; Dapprich, S.; Daniels, A. D.; Strain, M. C.; Farkas, O.; Malick, D. K.; Rabuck, A. D.; Raghavachari, K.; Foresman, J. B.; Ortiz, J. V.; Cui, Q.; Baboul, A. G.; Clifford, S.; Cioslowski, J.; Stefanov, B. B.; Liu, G.; Liashenko, A.; Piskorz, P.; Komaromi, I.; Martin, R. L.; Fox, D. J.; Keith, T.; Al-Laham, M. A.; Peng, C. Y.; Nanayakkara, A.; Challacombe, M.; Gill, P. M. W.; Johnson, B.; Chen, W.; Wong, M. W.; Gonzalez, C.; and Pople, J. A. *Gaussian 03*, Revision C.02; Gaussian, Inc.: Wallingford, CT, 2004.
(30) Gritzner, G.; Kuta, J. *Pure Appl. Chem.* **1984**, *56*, 461.
(31) *SAINT 6.02*; BRUKER-AXS, Inc.: Madison, WI, 1997−1999.
(32) Sheldrick, G. *SADABS*; Bruker AXS, Inc.: Madison,WI, 1999.
(33) Burla, M. C.; Camalli, M.; Carrozzini, B.; Cascarano, G. L.; Giacovazzo, C.; Polidori, G.; Spagna, R. *J. Appl. Crystallogr.* **2003**, *36*, 1103.
(34) *SHELXTL 6.14*; Bruker AXS, Inc.: Madison, WI, 2000−2003.